Journal of Materials Chemistry C

Accepted Manuscript

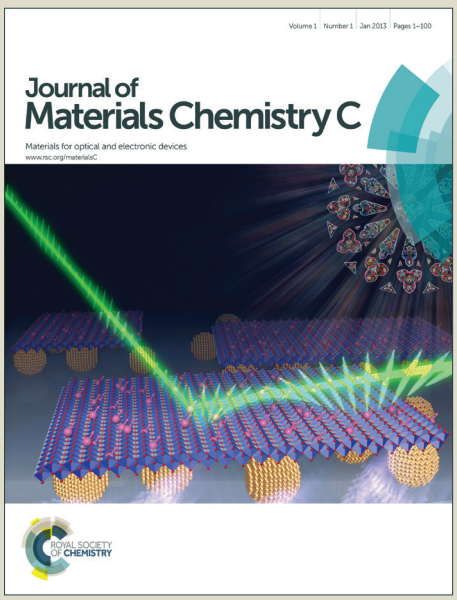

ROYAL SOCIETY OF CHEMISTRY

www.rsc.org/materialsC

Journal Name

RSCPublishing

ARTICLE

Enhanced Efficiency of Polymer Photovoltaic Cells via the Incorporation of a Water Soluble Naphthalene Diimide Derivative as Cathode Interlayer

Cite this: DOI: 10.1039/x0xx00000x

Received 00th January 2012,
Accepted 00th January 2012

DOI: 10.1039/x0xx00000x

www.rsc.org/

Kang Zhao,[a,b] Long Ye,*[b] Wenchao Zhao,[a] Shaoqing Zhang,[b] Huifeng Yao,[b] Bowei Xu,[b] Mingliang Sun*[a] and Jianhui Hou*[b]

In this contribution, a novel cathode interlayer material (NDIO) based on naphthalene diimide was successfully prepared by a facile two-step reaction from commercially available compounds. NDIO exhibited excellent water solubility, highly transparent in visible light region, and well-matched molecular energy levels. By incorporating this novel water processed cathode interlayer, a high power conversion efficiency of 9.51% was recorded in PBDT-TS1/$PC_{71}BM$-based polymer photovoltaic cell (PPC), and the value is nearly 2-fold of the device efficiency of PPC without cathode interlayer. More importantly, the insertion of the NDIO interlayer promotes the device efficiency of polymer/polymer photovoltaic cell based on PBDTTT-EFT/N2200 from 3.23% up to 5.77%. The successful applications in both polymer/PCBM and polymer/polymer blend-based inverted PPCs render NDIO a promising cathode interlayer for realizing aqueous processed polymer photovoltaics with high performance.

Introduction

In the past decade, much effort has been devoted to bulk-heterojunction (BHJ) polymer photovoltaic cells (PPCs) considering its unique advantages of low-cost, flexible, colorful and large-area fabrication.[1,2] Although conventional PPCs with the typical configuration of ITO/PEDOT:PSS/photoactive layer/Ca/Al exhibited outstanding power conversion efficiencies (*PCE*s).[3,4] Compared with the conventional PPC devices, inverted PPCs exhibit superior stability by using non-acidic anode interlayer transition metal oxides and air-stable anodes, such as Au or Ag, which can avoid the interfacial corrosion of ITO electrode caused by PEDOT:PSS and the instability caused by low-work-function metals.[5-9] A key component in high-performance inverted PPCs is the cathode interlayer which acts as effectively extracting electrons from active layer and then transferring electrons into indium tin oxide (ITO) electrode.[6-13] Although the *PCE*s of inverted PPC devices can be greatly improved by advanced cathode interlayers, most of the reported cathode interlayers need to be fabricated in organic solvents like ethanol, methanol, etc, which may not fulfill the requirements of human health, environment, and low cost. Therefore, for the future commercialization of inverted PPCs, it should intensely be desired for water processing cathode interlayers.

Recently, a variety of cathode interlayers based on polymer materials, for instance, PFN and its derivatives played important roles in achieving high performance inverted PPCs.[9-13] Compared with the polymer cathode interlayers, small molecules exhibited the advantages of both easy preparation and precise molecular weight due to its well-defined structure and relative small conjugated backbone.[14,15] Naphthalene diimide (NDI) has attracted considerable attention by chemists and have extensively been used as building block in small molecule acceptor materials[16] due to the adjustable energy levels, high electron mobility and easy synthesis. Although NDI-based small molecule cathode interlayers have not been reported yet, NDI might be a good choice for constituting novel small molecule cathode interlayer with excellent water solubility. In addition, most of the reported NDI derivatives can only be processed in organic solvents, which might be of unfavorable operation for economical and environmentally benign approach. Thus, the development of water-soluble naphthalene dimide materials acting as cathode interlayer of high-performance inverted PPCs will be desired for fundamental research and practical application.

Herein, we reported the synthesis of a novel water-soluble small molecule named NDIO (as shown in **Fig. 1a**), and its application in inverted PPC devices as a novel cathode interlayer. Polar group of amino N-oxide terminal substituent was

introduced as the side-chain of NDIO, so that the novel cathode interlayer could be prepared in aqueous solution. Remarkably, after inserting NDIO as cathode interlayer, the PBDT-TS1/$PC_{71}BM$-based inverted PPC (**Fig. 1b**) showed a considerable *PCE* of 9.51% under AM 1.5G 100 mW/cm^2 simulated solar light. Beyond the successful application in polymer:$PC_{71}BM$-based PPCs, this cathode interlayer works well in inverted polymer/polymer photovoltaic cells based on PBDTTT-EFT/N2200 blends, which afforded a high *PCE* of 5.77%. The water processing of NDIO is certainly beneficial to the low-cost and environmentally friendly manufacture of polymer photovoltaics.

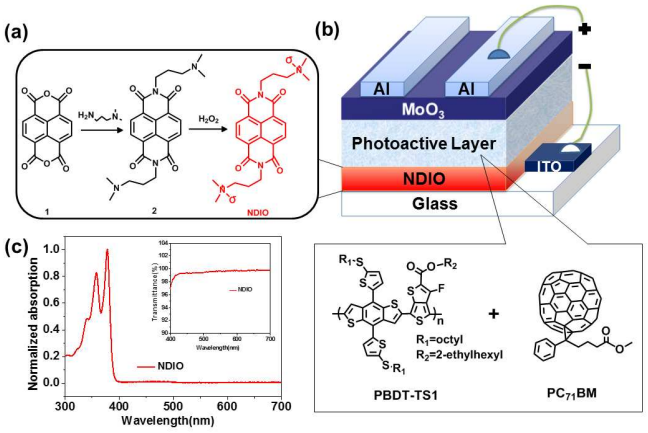

Fig. 1. (a) Preparation of NDIO; (b) Device configuration of the inverted PPC and chemical structures of PBDT-TS1 and $PC_{71}BM$; (c) Absorption spectra of NDIO in water solution. The insert shows the transmittance spectra of NDIO film on quartz substrate.

Results and discussion

The synthetic routes of NDIO are demonstrated in **Fig. 1a**. The final amino N-oxide product NDIO was prepared by a simple two-step reaction from commercial available compounds, 1, 4, 5, 8-naphthalenetetracarboxylic dianhydride and *N, N*-dimethyl-1,3-propane-diamine, with relatively high yield 75-80%. Owing to the polar *N, N*-dimethyl aminoxy end group, the compound NDIO is soluble in high polar organic solvents such as methanol and water, but insoluble in chlorinated solvents such as chlorobenzene and dichlorobenzene, so that the NDIO thin film is robust to support multi-layer solution processing. Moreover, the good solubility in water also endows NDIO with the potential of green manufacture, which should be of crucial significance for realizing commercialization of PPCs. The chemical structure of NDIO was characterized by ^{1}H NMR, ^{13}C NMR and N-MALDI-TOF-MS (or ESI-MS). The thermal behaviour of the NDIO was evaluated by thermal gravimetric analysis (TGA), and the curve was shown in **Fig. S1**.

Fig. 1c shows absorption spectrum of the NDIO in aqueous solution and the insert exhibits the transmittance spectrum of NDIO in solid thin film. The absorption band in the 300-400 nm range is typical of the NDI core and the polar amino *N*-oxide terminal group does not change the optical property of naphthalene diimide core. As to solid film, the UV-vis absorption onset of NDIO film is around 410 nm, which minimizes the optical loss in visible region as well as makes the cathode interlayer superior in modifying ITO electrode of inverted PPC. Moreover, from the transmittance spectrum, we can figure out that the light transmittance of NDIO film is in the range of 97-100% through the whole visible light region. This superior light transmittance is helpful to contribute to the efficient photon harvesting of the active layer, which is crucial for realizing high J_{sc} in inverted device. In addition, the operational stability of PPCs could be improved by absorbing ultraviolet light, which usually gives rise to photodegradation of organic materials.

To evaluate the highest occupied molecular orbital (HOMO) and the lowest unoccupied molecular orbital (LUMO) levels, the electrochemical properties of NDIO were investigated by cyclic voltammetry (CV). The CV plot of NDIO is showed in **Fig. S2**. Considering that the energy level of ferrocene (Fc) is 4.80 eV below the vacuum level, the LUMO level of NDIO was estimated to be -3.98 eV. The HOMO level of NDIO was calculated to be -7.00 eV from the equation: $E_{LUMO}=E_{HOMO}-E_g^{opt}$. As a result, the LUMO level of NDIO is suitable to collect electrons from the active layer and its HOMO level is deep enough to impede the hole carriers.

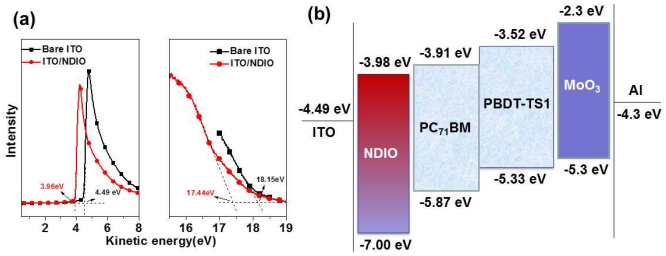

Fig. 2. (a) The inelastic secondary electron edge of ITO electrode with and without the NDIO film (the left panel) and the HOMO energy level region of ITO coated with and without NDIO thin film (the right panel); (b) the energy level diagram of each component in the inverted PPCs.

To investigate the effect of electronic properties of NDIO buffer layer on the photovoltaic performance, we carried out the ultraviolet photoelectron spectroscopy (UPS) measurement to study the energy levels of bare ITO and ITO covered by NDIO thin film. **Fig. 2a**) shows the inelastic secondary electron edge of ITO (indium tin oxide) electrode with and without the NDIO film (the left panel) and the HOMO level region of ITO coated with and without NDIO thin film (the right panel). The work function (WF) value of ITO (4.49 eV) measured by UPS is consistent with the reported results. With the modification by the NDIO thin film, the work function of ITO electrode can be reduced to 3.96 eV. The HOMO level of NDIO was obtained according to the following equation: $E_{HOMO}=(h\nu-E_{onset})+E_{cutoff}$, Where $h\nu$ is the incident photon energy ($h\nu$=21.22 eV) for He; E_{onset} is the onset value of HOMO energy region as shown in the right panel; E_{cutoff} is defined as the inelastic secondary electron edge obtained from the left panel. Thus, the HOMO level of NDIO buffer layer was -7.74 eV. The decrease of ITO work function may be attributed to the molecular dipole of NDIO (**Table S1**) formed at the interface between the NDIO cathode interlayer and ITO glass substrate. **Fig. 2b)** shows the corresponding energy-level diagram of each component in the inverted device, being indicative of WF modification by the NDIO interlayer. After modifying ITO with NDIO interlayer, the mismatch between the WF of ITO and $PC_{71}BM$ (3.91 eV) became smaller. In addition, NDIO owns sufficiently deep HOMO level. The admirable energy alignment makes it an ideal candidate as cathode interlayer to meet the requirements of extracting electron and impeding hole.

PBDT-TS1, a newly designed photovoltaic polymer exhibited excellent performance in the field of polymer photovoltaics due to the broad absorption, favorable molecular order, and high hole mobility.[17] Herein, PBDT-TS1/$PC_{71}BM$ blend (**Fig. 1b**) is selected as a model photoactive material to evaluate the applicability of NDIO in high performance polymer/fullerene photovoltaic devices. Polymer/fullerene solar cells based on PBDT-TS1/$PC_{71}BM$ blends were made in an inverted device configuration using transparent indium tin oxide (ITO)/cathode interlayer and reflective MoO_3/Al electrodes to collect electron and holes, respectively. The device with a configuration of ITO/photoactive layer/MoO_3/Al was also fabricated as control. **Fig. 3a** shows the *J-V* curves of inverted devices with NDIO cathode interlayer and without cathode layer, and the detailed performance parameters are summarized in **Table 1**. The PPC device without cathode interlayer only afford a moderate *PCE* of 5.14%. Impressively, the *PCE* of inverted device with NDIO buffer layer processed from aqueous solution reached 9.51% with a V_{oc} of 0.79 V, a J_{sc} of 18.02 mA/cm^2, and a *FF* of 66.82%. After modifying ITO with NDIO cathode interlayer, enhancements of V_{oc}, J_{sc}, and *FF* were simultaneously achieved, suggesting both an increased built-in field as a result of the interfacial dipole and a favorable electron transport due to the compatible organic-organic interface contact. Also, the device performance was investigated by the use of NDIO interlayer processed from methanol, and a slightly higher PCE of 9.74% was obtained in PBDT-TS1/$PC_{71}BM$ based PPCs (see **Table S2** and **Fig. S3**). Compared with the NDIO processed from aqueous solution, no distinct enhancement in PCE was observed as processing with methanol. As reported previously, alcohol processed interlayers like ZnO[2a], PDINO[14b,15], and PEIE[11b] performed well in polymer photovoltaic devices. We performed the PBDT-TS1/PCBM-based device using ZnO or PEIE instead of NDIO as cathode interlayer, and the photovoltaic characteristics are listed in **Table S3** and **Fig. S4**. It can be found that the *PCE* of PBDT-TS1/$PC_{71}BM$-based PPC device employing NDIO cathode interlayer is quite comparable with that PPC device using ZnO cathode interlayer (9.67%), and even slightly higher than that of device with PEIE cathode interlayer (9.32%). Apparently, the quality of NDIO film processed from water is comparable with film cast from methanol solution; this is favorable to green manufacture for PPCs commercialization. The comparable performance and green manufacture in water make NDIO great potential in practical application of inverted PPCs.

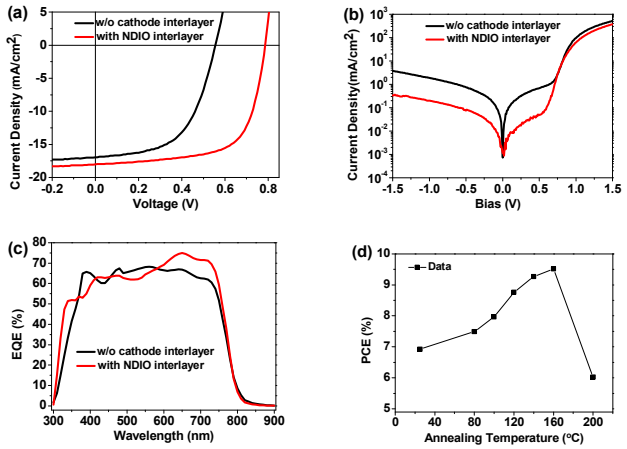

Fig. 3. Current density versus voltage (*J–V*) curves of the inverted PBDT-TS1/$PC_{71}BM$-based PPCs: (a) under the illumination of AM 1.5G, 100 mW/cm^2; (b) in the dark. (c) The corresponding external quantum efficiency (EQE) spectra of the inverted PPC devices with NDIO cathode interlayer and without cathode interlayer; (d) *J-V* characteristics of PBDT-TS1/$PC_{71}BM$-based PPCs employing annealed NDIO interlayers at different temperatures.

To understand the possible reasons for high photovoltaic performances of inverted PPCs, the *J-V* characteristics of inverted PPC devices with NDIO cathode interlayer and without cathode interlayer in the absence of illumination were performed. As can be seen from **Fig. 3b**, compared with device without cathode interlayer, the device modified with NDIO demonstrated an outstanding diode characteristic with lower leakage current, and the rectification ratio (the quotient of current density at ±1.5V), implying that the carrier recombination was suppressed by the NDIO cathode buffer layer. Generally, smaller series resistance (R_s) is favorable to improving photovoltaic parameters such as J_{sc} and *FF*. The increased J_{sc} and *FF* of the inverted device with NDIO interlayer can be partially attributed to the decrease of series resistance from 7.62 Ω·cm^2 for the control device to 4.19 Ω·cm^2, indicating an improved ohmic contact. The external quantum efficiency (*EQE*) spectra of the inverted device and the control device were also investigated, as shown in **Fig. 3c**. The PPC devices modified with NDIO showed much higher *EQE* compared with the device without cathode interlayer on the wavelength region from 600-800 nm. The calculated J_{sc} obtained by integration of the *EQE* curve for the PPC devices with NDIO cathode interlayer and without cathode interlayer were also consistent with the J_{sc} tested from *J-V* characteristics.

Table 1. Photovoltaic properties of various types of PPCs with NDIO cathode interlayer and without cathode interlayer under AM1.5G 100 mA/cm^2.

Photoactive Layer	Cathode Interlayer	V_{oc} (V)	J_{sc} (mA/cm^2)	*FF* (%)	*PCE* (%)
PBDT-TS1/$PC_{71}BM$	w/o	0.56	16.96	56.08	5.33
PBDT-TS1/$PC_{71}BM$	NDIO	0.79	18.02	66.82	9.51
PBDTTT-EFT/N2200	w/o	0.66	11.34	43.19	3.23
PBDTTT-EFT/N2200	NDIO	0.80	13.81	52.22	5.77

To investigate the effect of processing temperature on the NDIO layer, we put the ITO/NDIO substrate on the hot plate in nitrogen-filled glove box to carry out thermal annealing treatment at 80, 100, 120, 140, 160, and 200 °C for 10 min, respectively. The detailed device *PCE*s are summarized in the **Fig. 3d**. For the device without thermal annealing treatment on NDIO film, the *PCE* is 6.92%. When the NDIO interlayer was treated with different temperature (below 200 °C) annealing, all device *PCE*s enhanced to some extent. As the annealing temperature of NDIO layer increases from ambient temperature to 160 °C, the *PCE* increases from 6.92% to 9.51%. This is probably due to the thermal annealing process can remove the moisture in NDIO film, which improves the contact quality between the cathode

interlayer and photoactive layer. However, when the annealing temperature increases up to 200 °C, the NDIO compound will decompose (verified by TGA plot), which can destroy the film morphology so that the device performance drops to 6.03%. Therefore, the optimum annealing temperature of the NDIO interlayer is around 160 °C. The enhancement in J_{sc} of the inverted PPC device was investigated by varying the thickness of NDIO film atop the ITO glass substrate. Considering the thickness of NDIO film was too thin to be measured, we went in the opposite direction by controlling the concentration of NDIO in water. With the NDIO concentration ranging from 3 mg/mL to 10 mg/mL, the device *PCE* initially increase from 3 mg/mL to 8 mg/mL and then decrease with the increase of concentration (**Fig. S5**). The optimal NDIO concentration is 8 mg/ml in water. When the concentration is too low, the NDIO layer may only partially cover the ITO surface so that the WF of ITO may be not well modified, resulting in poor ohmic contact with the active layer. When the NDIO layer is too thick theoretically, the NDIO film will hinder not only the absorption of incident light but also the electron extraction and collection of cathode.

Thereafter, atomic force microscopy (AFM) measurement in tapping mode was carried out to probe the surface morphology of the optimum NDIO film on ITO substrate. The AFM characterization of bare ITO substrate was also performed as control. **Fig. 4** shows the surface morphology of NDIO film with the control ITO glass. Apparently, the ITO glass covered by thin NDIO film exhibits much lower root-mean-square roughness (R_q=2.09 nm) than the bare ITO (R_q=3.33 nm). Clearly, the introduction of NDIO as cathode interlayer may facilitate the contact quality with PBDT-TS1:$PC_{71}BM$ active layer and decreases the contact resistance so as to improve charge collection effectively.

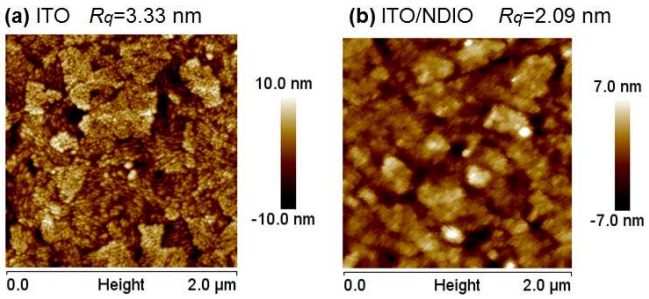

Fig. 4. Tapping-mode AFM height images of the control bare ITO glass (a) and the ITO glass covered by NDIO film (b).

Recently, all polymer photovoltaics utilizing conjugated polymers as both donor and acceptor materials are attracting renewed attention and regarded as a potential candidate to replace polymer/fullerene photovoltaic devices.[18-22] Particularly, all polymer photovoltaic devices with considerable power conversion efficiencies in excess of 4% were achieved in several groups by the use of the high electron mobility polymer N2200 as acceptor material.[21-25] To explore the potential of NDIO in other types of polymer photovoltaics, we also utilized this cathode interlayer in polymer/polymer photovoltaic devices, in which PBDTTT-EFT/N2200 blend was selected as photoactive layer (**Fig. 5a**). As shown in **Fig. 5b**, the polymer/polymer photovoltaic cell achieved simultaneously increased V_{oc} (0.80 V vs 0.66 V), J_{sc} (13.81 mA/cm² vs 11.34 mA/cm²), and *FF* (52.22% vs 43.19%), which lead to a ~80% enhancement in the overall device efficiency. Therefore, the aforementioned results demonstrated that NDIO cathode interlayer shows great potentials and good applicability in two types of inverted PPCs, i.e., polymer/PCBM and polymer/polymer photovoltaic devices.

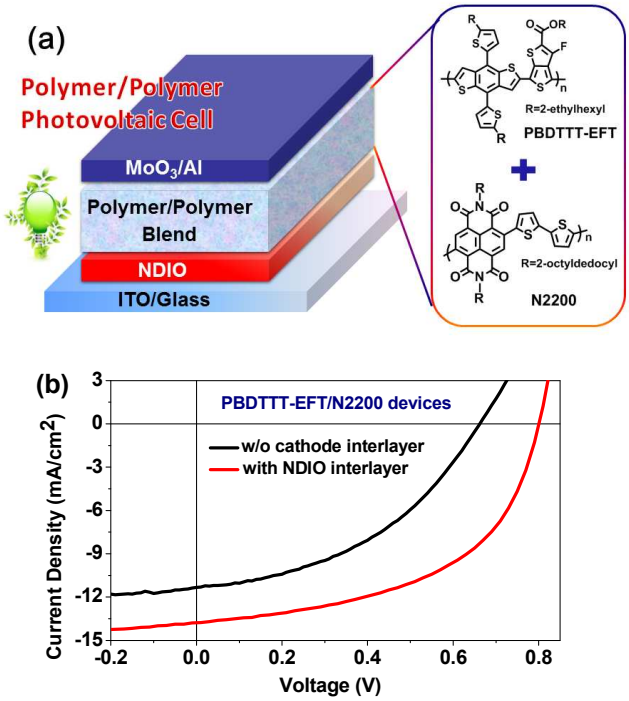

Fig. 5. (a) Schematic illustration of polymer/polymer photovoltaic cell and molecular structures of PBDTTT-EFT and N2200; (b) *J-V* characteristics of polymer/polymer photovoltaic cells based on PBDTTT-EFT/N2200 with NDIO cathode interlayer and without cathode interlayer.

Experimental

Materials and Instruments. The 1, 4, 5, 8-naphthalenetetracarboxylic dianhydride was purchased from J&K Co. Ltd. The *N, N*-dimethyl-1, 3-propane diamine was purchased from TCI corporation. $PC_{71}BM$ and the polymer acceptor N2200 (Mn=138.1 KDa; PDI=2.37) were purchased from Solarmer Energy Inc. PBDT-TS1[16] and PBDTTT-EFT (M_n=26.79 KDa; PDI=2.51)[26] were synthesized in our laboratory following the previous works. The PEDOT:PSS (Heraeus Clevios™ P VP AI 4083) and high purity Al are commercial available products. All of the commercially available compounds and reagents were used without any further purification. ^{1}H NMR and ^{13}C NMR spectra were measured on a Bruker advance II spectrometer with d-chloroform, D_2O and methanol-d4 as the solvent and tetramethylsilane as the internal reference. Ultraviolet-visible absorption spectra were tested on a TU-1901 UV-vis spectrophotometer. Elemental analyses were implemented on a flash EA 1112 elemental analyzer. The electrochemical cyclic voltammetry was carried out on a specification for CHI650D Electrochemical Workstation. Atomic force microscopy (AFM) was conducted on a Nanoscope V (Vecco) AFM by tapping mode. TGA measurement was performed on TGA-2050 from TA Instruments, Inc. UPS measurement were analysed on Thermo Scientific ESCALab 250Xi. The gas discharge lamp was used for UPS, with helium gas admitted and the HeI (21.22 eV) emission line employed. The

helium pressure in the analysis chamber during analysis was about 2E-8 mbar. The data were acquired with -10V bias.

The *J-V* characteristics of the solar cell devices were measured under one sun, AM 1.5G (100 mW/cm^2), using a XES-70S1 (SAN-EI ELECTRIC CO., Ltd.) solar simulator (AAA grade, 70mm ×70 mm photobeam size) with 2×2 cm silicon reference cell (KG3 filter) purchased from Enli Technology Co., Ltd.[27] The external quantum efficiency (EQE) was measured by a Solar Cell Spectral Response Measurement System QE-R3011 (Enli Technology Co., Ltd.). During the *J-V* measurements, a shadow mask with a single aperture (4.15 mm^2) was placed onto the devices in order to accurately define the photoactive area.

Synthesis of Compound 2. 1, 4, 5, 8-naphthalenetetracarboxylic dianhydride（4.36 g, 0.01 mol）and corresponding *N,N*-dimethyl-1,3-propane diamine (3 mL, 0.021 mol) were suspended in 100 ml of dimethylformamide (DMF) in a 250 ml two-neck round-bottom flask. To this suspension, Et_3N (1 mL) was added and allowed to reflux for 12 h in air atmosphere. After cooling the reaction mixture to ambient temperature, the precipitate was filtered and recrystallized from ethanol. Light yellow solid crystal was obtained with a yield of 75%. N-MALDI-TOF-MS m/z: [M] calcd for $C_{24}H_{28}N_4O_4$, 436.21; found 436.30. ^{1}H NMR (400 MHz, $CDCl_3$, δ): 8.75 (s, 4H), 4.26 (t, 4H), 2.46 (t, 4H), 2.25 (s, 12H), 1.94 (m, 4H). ^{13}C NMR (300 MHz, $CDCl_3$, δ):162.83, 130.89, 126.68, 126.64, 57.20, 45.35, 39.34, 25.95. Anal. Calcd for $C_{24}H_{28}N_4O_4$: C, 66.04; H, 6.47; N, 12.84; found: C, 66.19; H, 6.47; N, 12.85.

Synthesis of NDIO. Compound 2 (200 mg, 0.459 mmol) and methanol (20 mL) were suspended in a 100 mL two necked round-bottom flask. To the stirred suspension hydrogen peroxide (30 percent, 1 mL) was added dropwise under the protection of an argon atmosphere. The reaction mixture was stirred violently at ambient temperature for 2 days. Then the resulting mixture was concentrated under reduced pressure, precipitated from acetic ether, and washed sequentially with acetic ether and tetrahydrofuran each three times. The powder product (172 mg) was obtained with a yield of 80%. ESI-MS m/z: $[M+H]^+$ calcd. for $C_{24}H_{28}N_4O_6$, 468.20; found, 469.5. ^{1}H NMR (400 MHz, D_2O, δ): 8.59 (s, 4H), 4.27 (t, 4H), 3.48 (t, 4H), 3.20 (s, 12H), 2.36 (m, 4H).^{13}C NMR (300 MHz, MeOD-d4, δ):162.92, 130.29, 126.38, 126.33, 67.95, 57.19, 37.60, 22.25.

Fabrication of Inverted Polymer/PCBM photovoltaic Cells. The inverted PPCs were fabricated with the structure of glass/ITO/NDIO/photoactive layer/MoO_3/Al. The NDIO solution was spin-coated at 3000 rpm for 60 s on the pre-cleaned ITO electrode. Next, the NDIO film was baked at 160 ^{o}C for 10 min. A solution containing a mixture of PBDT-TS1/$PC_{71}BM$ (1:1.5 wt/wt) in chlorobenzene with a total concentration of 25 mg/ml was prepared and stirred for several hours for complete dissolution. The additives (3 vol% DIO) were added to the blend solution before spin-coating. Then the blend solution was spin-coated on top of the NDIO layer to produce a 100-nm-thick active layer. After that, the substrate was transferred to a vacuum chamber and a 10 nm of MoO_3 layer was thermally deposited atop the photoactive layer under a shadow mask in a base pressure of ca. 3×10^{-4} Pa. Finally, 100 nm of Al layer was thermally deposited on the top of MoO_3 layer in vacuum. The typical device area is 4.15 mm^2. The deposition of ZnO and PEIE layer were following previous works by Yang *et al.*[2a] and Zhou et al.[11b], respectively.

Fabrication of Inverted Polymer/polymer Photovoltaic Cells. The preparation method of devices is identical with that of polymer:PCBM devices besides of the photoactive layer. The blend solution containing a mixture of PBDTTT-EFT/N2200 (1:1 wt/wt) with a total concentration of 10 mg/ml in chlorobezene was spin-coated at 2000 rpm for 60 s, and processing additive was not introduced at all.[23]

Conclusions

In this study, a novel water-soluble naphthalene dimide derivative NDIO was designed, synthesized, and utilized as cathode interlayer by aqueous solution processing for inverted PPC devices. NDIO thin film meet the four requirements for efficient cathode interlayer: 1) high transparency for minimizing the loss of incident photons; 2) suitable work-function for efficient electron collection; 3) low roughness for excellent interface contact; 4) easily processed by water. The photovoltaic performance of inverted PPC devices showed significantly increase by utilizing the NDIO interlayer due to the superior ability of NDIO in regulating energy level of ITO electrode. Based on spin-coating of NDIO film from aqueous solution, a considerable PCE of 9.51% was achieved in inverted PPC based on PBDT-TS1/$PC_{71}BM$. Simultaneous improvements of the J_{sc}, V_{oc} and *FF* values resulted in a PCE enhancement from 5.33% to 9.51% in polymer/PCBM photovoltaic cell and from 3.23% to 5.77% in polymer/polymer photovoltaic cell with the insertion of NDIO as cathode interlayer. Both the significant enhancements of PCE values and the green manufacture in water make the naphthalene dimide derivative NDIO great potential in practical application of inverted PPCs. Integrating the green processing of both photoactive layers[28] and interlayers, green and high efficiency polymer photovoltaics will be soon achieved.

Acknowledgements

The authors would like to acknowledge the financial support from the National Basic Research Program 973 (2014CB643501), the NSFC (Nos. 91333204, 51261160496), and the Chinese Academy of Sciences (No. XDB12030200). M. L. Sun gratefully acknowledges financial supports from the NSFC (21274134) and New Century Excellent Talents in University (NCET-11-0473).

Notes and references

[a] Institute of Material Science and Engineering, Ocean University of China, Qingdao 266100, P. R. China

[b] State Key Laboratory of Polymer Physics and Chemistry, Beijing National Laboratory for Molecular Sciences, Institute of Chemistry, Chinese Academy of Sciences, Beijing 100190, P. R. China

*E-mail: mlsun@ouc.edu.cn (Dr. M. Sun); hjhzlz@iccas.ac.cn (Prof. J. Hou); yelong@iccas.ac.cn (Dr. L. Ye), Tel: +86-10-82615900.

† Electronic Supplementary Information (ESI) available: Additional Cyclic Voltammetry data, DFT calculation, and device performances under various circumstances. See DOI: 10.1039/b000000x/

1. (a) L. Dou, J. You, Z. Hong, Z. Xu, G. Li, R. A. Street and Y. Yang, *Adv Mater*, 2013, **25**, 6642-6671; (b) F. Wang, Z. a. Tan and Y. Li, *Energy Environ. Sci.*, 2015, **8**, 1059-1091; (c) C. Duan, K. Zhang, C. Zhong, F. Huang and Y. Cao, *Chem. Soc. Rev.*, 2013, **42**, 9071-9104; (d) Z. He, H. Wu and Y. Cao, *Adv. Mater.*, 2014, **26**, 1006-1024. (e) L. Ye, S. Zhang, L. Huo, M. Zhang and J. Hou, *Acc. Chem. Res.*, 2014, **47**, 1595-1603.
2. (a) J. You, L. Dou, K. Yoshimura, T. Kato, K. Ohya, T. Moriarty, K. Emery, C.-C. Chen, J. Gao, G. Li and Y. Yang, *Nat. Commun.*, 2013, **4**, 1446; (b) K. S. Chen, J. F. Salinas, H. L. Yip, L. J. Huo, J. H. Hou and A.

K. Y. Jen, *Energy Environ. Sci.*, 2012, **5**, 9551-9557; (c) L. J. Zuo, C. Y. Chang, C. C. Chueh, S. H. Zhang, H. Y. Li, A. K. Y. Jen and H. Z. Chen, *Energy Environ. Sci.*, 2015, **8**, 1712-1718; (d) S. Zhang, L. Ye, W. Zhao, B. Yang, Q. Wang and J. Hou, *Sci. China Chem.*, 2015, **58**, 248-256.

3. (a) P. Cheng, Y. Li and X. Zhan, *Energy Environ. Sci.*, 2014, **7**, 2005-2011; (b) P. Cheng, C. Yan, Y. Li, W. Ma and X. Zhan, *Energy Environ. Sci.*, 2015, **8**, 2357-2364; (c) L. Ye, S. Zhang, W. Ma, B. Fan, X. Guo, Y. Huang, H. Ade and J. Hou, *Adv. Mater.*, 2012, **24**, 6335-6341; (d) W. Zhao, L. Ye, S. Zhang, B. Fan, M. Sun and J. Hou, *Sci. Rep.*, 2014, **4**, 6570.
4. (a) L. M. Chen, Z. R. Hong, G. Li and Y. Yang, *Adv. Mater.*, 2009, **21**, 1434-1449; (b) H. Zhang, L. Ye and J. Hou, *Polym. Int.*, 2015, **64**, 957-962.
5. H. L. Yip and A. K. Y. Jen, *Energy Environ. Sci.*, 2012, **5**, 5994-6011.
6. (a) Z. A. Tan, W. Q. Zhang, Z. G. Zhang, D. P. Qian, Y. Huang, J. H. Hou and Y. F. Li, *Adv. Mater.*, 2012, **24**, 1476-1481.; (b) X. H. Li, W. C. H. Choy, L. J. Huo, F. X. Xie, W. E. I. Sha, B. F. Ding, X. Guo, Y. F. Li, J. H. Hou, J. B. You and Y. Yang, *Adv. Mater.*, 2012, **24**, 3046-3052; (c) S. H. Liao, H. J. Jhuo, P. N. Yeh, Y. S. Cheng, Y. L. Li, Y. H. Lee, S. Sharma and S. A. Chen, *Sci. Rep.*, 2014, **4**, 6813.
7. (a) Y. Liu, J. Zhao, Z. Li, C. Mu, W. Ma, H. Hu, K. Jiang, H. Lin, H. Ade and H. Yan, *Nat. Commun.*, 2014, **5**, 5293; (b) J. D. Chen, C. Cui, Y. Q. Li, L. Zhou, Q. D. Ou, C. Li, Y. Li and J. X. Tang, *Adv. Mater.*, 2015, **27**, 1035-1041; (c) L. Nian, W. Zhang, N. Zhu, L. Liu, Z. Xie, H. Wu, F. Würthner and Y. Ma, *J. Am. Chem. Soc.*, 2015, **137**, 6995-6998.
8. T. L. Nguyen, H. Choi, S. J. Ko, M. A. Uddin, B. Walker, S. Yum, J. E. Jeong, M. H. Yun, T. J. Shin, S. Hwang, J. Y. Kim and H. Y. Woo, *Energy Environ. Sci.*, 2014, **7**, 3040-3051.
9. J. H. Seo, A. Gutacker, Y. M. Sun, H. B. Wu, F. Huang, Y. Cao, U. Scherf, A. J. Heeger and G. C. Bazan, *J. Am. Chem. Soc.*, 2011, **133**, 8416-8419.
10. (a) B. Zhao, Z. He, X. Cheng, D. Qin, M. Yun, M. Wang, X. Huang, J. Wu, H. Wu and Y. Cao, *J. Mater. Chem. C*, 2014, **2**, 5077-5082; (b) Z. He, B. Xiao, F. Liu, H. Wu, Y. Yang, S. Xiao, C. Wang, T. P. Russell and Y. Cao, *Nat. Photonics*, 2015, **9**, 174-179.
11. (a) C. Gu, Y. Chen, Z. Zhang, S. Xue, S. Sun, C. Zhong, H. Zhang, Y. Lv, F. Li, F. Huang and Y. Ma, *Adv. Energy Mater.*, 2014, **4**: 1301771; (b) Y. H. Zhou, C. Fuentes-Hernandez, J. Shim, J. Meyer, A. J. Giordano, H. Li, P. Winget, T. Papadopoulos, H. Cheun, J. Kim, M. Fenoll, A. Dindar, W. Haske, E. Najafabadi, T. M. Khan, H. Sojoudi, S. Barlow, S. Graham, J. L. Bredas, S. R. Marder, A. Kahn and B. Kippelen, *Science*, 2012, **336**, 327-332.
12. (a) T. B. Yang, M. Wang, C. H. Duan, X. W. Hu, L. Huang, J. B. Peng, F. Huang and X. Gong, *Energy Environ. Sci.*, 2012, **5**, 8208-8214; (b) S. Liu, K. Zhang, J. Lu, J. Zhang, H.-L. Yip, F. Huang and Y. Cao, *J. Am. Chem. Soc.*, 2013, **135**, 15326-15329.
13. (a) X. Guo, M. Zhang, W. Ma, L. Ye, S. Zhang, S. Liu, H. Ade, F. Huang and J. Hou, *Adv. Mater.*, 2014, **26**, 4043-4049; (b) P. Liu, K. Zhang, F. Liu, Y. Jin, S. Liu, T. P. Russell, H.-L. Yip, F. Huang and Y. Cao, *Chem. Mater.*, 2014, **26**, 3009-3017.
14. (a) W. Zhang, Y. Wu, Q. Bao, F. Gao and J. Fang, *Adv. Energy Mater.*, 2014, **4**: 1400359; (b) Z.-G. Zhang, B. Qi, Z. Jin, D. Chi, Z. Qi, Y. Li and J. Wang, *Energy Environ. Sci.*, 2014, **7**, 1966-1973.
15. (a) Y. Lin, J. Wang, Z.-G. Zhang, H. Bai, Y. Li, D. Zhu and X. Zhan, *Adv. Mater.*, 2015, **27**, 1170-1174; (b) Y. Z. Lin, Z. G. Zhang, H. T. Bai, J. Y. Wang, Y. H. Yao, Y. F. Li, D. B. Zhu and X. W. Zhan, *Energy Environ. Sci.*, 2015, **8**, 610-616.
16. Y. Liu, L. Zhang, H. Lee, H.-W. Wang, A. Santala, F. Liu, Y. Diao, A. L. Briseno and T. P. Russell, *Adv. Energy Mater.*, 2015, DOI: 10.1002/aenm.201500195.
17. (a) L. Ye, S. Zhang, W. Zhao, H. Yao and J. Hou, *Chem. Mater.*, 2014, **26**, 3603-3605; (b) L. Ye, K. Sun, W. Jiang, S. Zhang, W. Zhao, H. Yao, Z. Wang and J. Hou, *ACS Appl. Mater. Interfaces*, 2015, **7**, 9274-9280.
18. (a) C. R. McNeill and N. C. Greenham, *Adv. Mater.*, 2009, **21**, 3840-3850; (b) A. Facchetti, *Mater. Today*, 2013, **16**, 123-132; (c) Y. Lin and X. Zhan, *Mater. Horiz.*, 2014, **1**, 470-488.
19. (a) X. Zhan, Z. a. Tan, B. Domercq, Z. An, X. Zhang, S. Barlow, Y. Li, D. Zhu, B. Kippelen and S. R. Marder, *J. Am. Chem. Soc.*, 2007, **129**, 7246-7247; (b) X. W. Zhan, A. Facchetti, S. Barlow, T. J. Marks, M. A. Ratner, M. R. Wasielewski and S. R. Marder, *Adv. Mater.*, 2011, **23**, 268-284; (c) X. Zhao and X. Zhan, *Chem. Soc. Rev.*, 2011, **40**, 3728-3743.
20. (a) H. Yan, B. A. Collins, E. Gann, C. Wang, H. Ade and C. R. McNeill, *ACS Nano*, 2011, **6**, 677-688; (b) E. Zhou, J. Cong, K. Hashimoto and K. Tajima, *Adv. Mater.*, 2013, **25**, 6991-6996; (c) P. Cheng, L. Ye, X. Zhao, J. Hou, Y. Li and X. Zhan, *Energy Environ. Sci.*, 2014, **7**, 1351-1356; (d) W. Li, W. S. C. Roelofs, M. Turbiez, M. M. Wienk and R. A. J. Janssen, *Adv. Mater.*, 2014, **26**, 3304-3309.
21. (a) Y. Zhou, T. Kurosawa, W. Ma, Y. Guo, L. Fang, K. Vandewal, Y. Diao, C. Wang, Q. Yan, J. Reinspach, J. Mei, A. L. Appleton, G. I. Koleilat, Y. Gao, S. C. B. Mannsfeld, A. Salleo, H. Ade, D. Zhao and Z. Bao, *Adv. Mater.*, 2014, **26**, 3767-3772; (b) Y.-J. Hwang, T. Earmme, B. A. E. Courtright, F. N. Eberle and S. A. Jenekhe, *J. Am. Chem. Soc.*, 2015, **137**, 4424-4434.
22. (a) C. Mu, P. Liu, W. Ma, K. Jiang, J. Zhao, K. Zhang, Z. Chen, Z. Wei, Y. Yi, J. Wang, S. Yang, F. Huang, A. Facchetti, H. Ade and H. Yan, *Adv. Mater.*, 2014, **26**, 7224-7230; (b) H. Kang, M. A. Uddin, C. Lee, K.-H. Kim, T. L. Nguyen, W. Lee, Y. Li, C. Wang, H. Y. Woo and B. J. Kim, *J. Am. Chem. Soc.*, 2015, **137**, 2359-2365.
23. D. Mori, H. Benten, I. Okada, H. Ohkita and S. Ito, *Energy Environ. Sci.*, 2014, **7**, 2939-2943.
24. (a) C. Lee, H. Kang, W. Lee, T. Kim, K. H. Kim, H. Y. Woo, C. Wang and B. J. Kim, *Adv. Mater.*, 2015, **27**, 2466-2471; (b) L. Ye, X. Jiao, M. Zhou, S. Zhang, H. Yao, W. Zhao, A. Xia, H. Ade and J. Hou, *Adv. Mater.*, 2015, DOI:10.1002/adma.201503218.
25. J. W. Jung, J. W. Jo, C. C. Chueh, F. Liu, W. H. Jo, T. P. Russell and A. K. Jen, *Adv. Mater.*, 2015, **27**, 3310-3317.
26. (a) S.-H. Liao, H.-J. Jhuo, Y.-S. Cheng and S.-A. Chen, *Adv. Mater.*, 2013, **25**, 4766-4771; (b) S. Zhang, L. Ye, W. Zhao, D. Liu, H. Yao and J. Hou, *Macromolecules*, 2014, **47**, 4653-4659.
27. L. Ye, C. Zhou, H. Meng, H.-H. Wu, C.-C. Lin, H.-H. Liao, S. Zhang and J. Hou, *J. Mater. Chem. C*, 2015, **3**, 564-569.
28. W. Zhao, L. Ye, S. Zhang, M. Sun and J. Hou, *J. Mater. Chem. A*, 2015, **3**, 12723-12729.

Table of Content

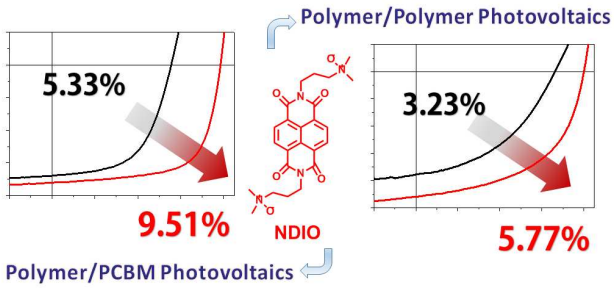

A novel water-soluble naphthalene dimide derivative was utilized as cathode interlayers for two types of high performance polymer photovoltaic cells.